

## **Exchange spring driven spin flop transition in $\text{ErFe}_2/\text{YFe}_2$ multilayers**

K. N. Martin, K. Wang, G. J. Bowden and P. A. J. de Groot

*School of Physics and Astronomy, University of Southampton, SO17 1BJ, United Kingdom*

J. P. Zimmermann and H. Fangohr

*Computational Engineering and Design Group, School of Engineering Sciences, University of Southampton, SO17 1BJ, United Kingdom*

R. C. C. Ward

*Clarendon Laboratory, Oxford University, OX1 3PU, United Kingdom*

PACs numbers: 75.70 Cn, 75.50 Gg, 75.30 Gw, 75.40 Mg

### **Abstract.**

Magnetization loops for (110) MBE grown  $\text{ErFe}_2/\text{YFe}_2$  multilayer films are presented and discussed. The magnetocrystalline easy axis for the Er layers is parallel to a  $\langle 111 \rangle$  type crystal axis, with the out of plane  $\langle 111 \rangle$  axes favoured by the strain. For fields applied along the (110) crystal growth axis, out-of-plane magnetic exchange springs are set up in the magnetically soft  $\text{YFe}_2$  layers. For multilayer films that display exchange spring dominated reversal at low temperatures, there is a cross-over temperature above which there are additional transitions at high fields. These features are interpreted using micro-magnetic modelling. At sufficiently high fields, applied perpendicular to the multilayer film plane, the energy is minimized by an exchange spring driven multilayer spin flop. In this state, the average magnetization of the  $\text{ErFe}_2$  layers switches into a nominally hard in-plane  $\langle 111 \rangle$  axis, perpendicular to the applied field.

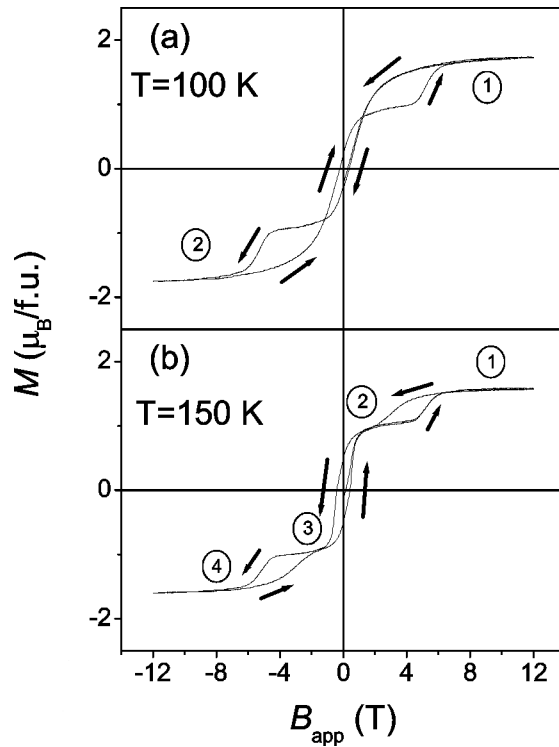


**Fig. 1.** Hysteresis curves obtained for  $[\text{ErFe}_2(50 \text{ \AA})/\text{YFe}_2(150 \text{ \AA})] \times 20$  at (a) 100 K and (b) 150 K. The arrows indicate the direction in which the field is being swept.  $B_{\text{app}}$  is parallel to the  $[110]$  growth axis.

Research into exchange spring magnets has flourished in recent years.<sup>1-7</sup> Early work focussed on potential applications in permanent magnets.<sup>3,4</sup> But more recently, exchange spring media have been proposed for magnetic data storage.<sup>5-7</sup> Epitaxial RE-Fe superlattices (RE is a heavy rare earth), grown by molecular beam epitaxy (MBE), have proved to be ideal model systems in which to study exchange spring phenomena.<sup>2,8</sup> In these MBE-grown multilayers, exchange springs are set up in the magnetically soft YFe<sub>2</sub> layers. They display a rich variety of features, including exchange spring induced giant magnetoresistance.<sup>9</sup> But more features continue to be discovered. For example, X-ray Magnetic Circular Dichroism (XMCD) studies on a YFe<sub>2</sub> dominated DyFe<sub>2</sub>/YFe<sub>2</sub> system reveal complex magnetization reversal processes.<sup>10</sup> In this Letter, we report complex magnetic re-orientations in ErFe<sub>2</sub>/YFe<sub>2</sub> superlattices.

ErFe<sub>2</sub>/YFe<sub>2</sub> superlattices are characterized by strong (~600 K) Fe-Fe ferromagnetic exchange, with AF-coupling between the Er and Fe moments. In zero field, the superlattices can be described as man-made AF magnets with the net magnetizations in the ErFe<sub>2</sub> and YFe<sub>2</sub> layers opposite to each other. The magnetocrystalline easy axes in the hard ErFe<sub>2</sub> layers are parallel to the <111> type crystal axes, however the strain induced during crystal growth favours an easy axis nearly along the out of plane <111> axes. At low temperatures, magnetic reversal in YFe<sub>2</sub> dominated samples is found to be dominated by exchange springs within the YFe<sub>2</sub> layers. There is just one irreversible switching of the hard layers. But at higher temperatures significant changes occur. Micro-magnetic modelling reveals that this can be attributed to differing spin configurations associated with the anisotropy energy of the ErFe<sub>2</sub> layers. In particular, a *multilayer spin flop state* is found to yield the lowest energy in high fields applied perpendicular to the multilayer plane. In this state the average magnetization of the ErFe<sub>2</sub> layers points nearly perpendicular to the applied field direction. The work illustrates a class of spin flop (SF) transitions driven by magnetic exchange springs in magnetically soft layers. They are generically different from the SF transitions witnessed in the man-made AF multilayers, such as (Co/Re).<sup>11</sup>

The ErFe<sub>2</sub>/YFe<sub>2</sub> superlattices were grown by MBE, following a procedure described elsewhere.<sup>12</sup> A 100 Å Nb buffer and 20 Å Fe seed layer were deposited onto epi-prepared (11 $\bar{2}$ 0)sapphire substrate of dimensions 10 mm×12 mm. The Laves phase material was grown in (110) orientation, with the major axes parallel to those of Nb. This was achieved by co-deposition of elemental fluxes at a substrate temperature of 400°C. The magnetic data was obtained using a vibrating sample magnetometer, using applied fields  $B_{app}$  of up to 12 T, within a temperature range of 10 to 310 K.<sup>13</sup> In all cases the field was applied along the [110] growth-axis, perpendicular to the plane of the multilayer. Micro-magnetic 1D simulations were performed using the finite difference method with the Object Oriented Micro-magnetic Framework (OOMMF) software.<sup>14</sup>

In this letter we highlight the unusual magnetic behaviour of the near compensated [ErFe<sub>2</sub>(50 Å)/YFe<sub>2</sub>(150 Å)]×20 (SL1) and [ErFe<sub>2</sub>(50 Å)/YFe<sub>2</sub>(100 Å)]×27 (SL2) multilayer films. Two magnetisation curves for SL1 can be seen in Fig. 1(a,b). At temperatures below 100 K, the measured coercivity appears negative, a familiar feature of exchange spring multilayers with relatively thick soft magnetic layers.<sup>15</sup> This is due to the unwinding of the exchange spring in the YFe<sub>2</sub> layers, which results in the average soft layer magnetisation

pointing opposite to the applied field. However, as the temperature is raised above a crossover temperature  $T_{CO}$ , the coercivity becomes positive and the character of the hysteresis loop changes. For SL1 (SL2),  $T_{CO}$  is  $\sim 130$  K ( $\sim 180$  K), respectively. Below  $T_{CO}$  there is just one irreversible step in the magnetization curve, but at higher temperatures there are three. This unusual behaviour was confirmed using partial hysteresis loops, carried out above and below  $T_{CO}$ . For SL1 at 100 K (Fig. 1a), reversal involves just one irreversible switching of the  $\text{ErFe}_2$  layers, at  $\sim 4.5$  T. This is similar to the process of magnetic reversal by exchange springs in  $\text{DyFe}_2/\text{YFe}_2$  multilayers described elsewhere,<sup>16</sup> except that the applied field is now parallel to the [110] crystallographic axis and the spin-configurations are out of plane. But at 150 K (Fig. 1b) there are three irreversible steps in the magnetic loop, as  $B_{app}$  is swept from 12 T to -12 T. The first irreversible step begins when the applied field is reduced below 5 T. The second step is associated primarily with the change in polarity of  $B_{app}$ , with a positive coercivity of 0.4 T. The third step begins at an applied field of -4.5 T.

We attribute these changes in the character of the hysteresis loop to differing spin configurations that minimize the total energy of the multilayer. The three contributors are the Fe-Fe exchange energy, the Er anisotropy energy, and the Zeeman energy. The magneto-crystalline energy is calculated using the phenomenological constants  $K_1$ ,  $K_2$  and  $K_3$  of Atzmony and Dariel,<sup>17</sup>. For Er,  $K_1$ - $K_3$  favour  $\langle 111 \rangle$ -type cubic axes. However the magneto-elastic strain term ( $b_2 \varepsilon_{xy}$ ) (see Mougín *et al.*<sup>18,19</sup>) favours the out of plane [110] crystal growth axis. As a result, the out-of plane eg. [111] or  $[11\bar{1}]$ -axes are preferred directions of magnetization. Both the anisotropy constants and the strain term are, of course, temperature dependent, with the former falling more rapidly with increasing temperature. In Fig. 2(a,b) we show the calculated anisotropy surfaces for the  $\text{ErFe}_2$  layers at 100 K and 200 K. In producing these plots, the anisotropy energy has been shifted by a constant, so that the energy remains positive over the entire surface. At 100 K the energy difference between the maximum and minimum energies is  $3.47 \times 10^6 \text{ Jm}^{-3}$ , whereas at 200 K it is  $0.587 \times 10^6 \text{ Jm}^{-3}$ , nearly an order of magnitude smaller. In both cases however, the global minimum is always along an out of plane  $\langle 111 \rangle$ -axis. For the discussion below, we shall assume that it is the  $[11\bar{1}]$  axes. Nonetheless, there are four local minima corresponding to the alignment of the  $\text{ErFe}_2$  magnetisation along in-plane  $\langle 111 \rangle$ -axes. For these directions, at 200 K, the energy is  $2.71 \times 10^5 \text{ Jm}^{-3}$  above the global minimum. The arrows shown in Fig 2, represent the average direction in which the  $\text{ErFe}_2$  magnetic moments point, as determined by micro-magnetic modelling. The arrows are numbered to correspond with the numbers on the hysteresis curves of Fig. 1. Finally, the calculated magnetization curves for the SL1 film can be seen in Fig. 3(a,b). It should be remarked that that the coercive fields predicted by the model are high. The 1D micro-magnetic model does not take into account formation of in-plane domain walls, and hence over-estimates the field required to switch the  $\text{ErFe}_2$  moments.<sup>20,21</sup> To some extent this can be compensated by using parameters  $K_1$ - $K_3$  for a higher temperature, which is why we have selected 200 K.

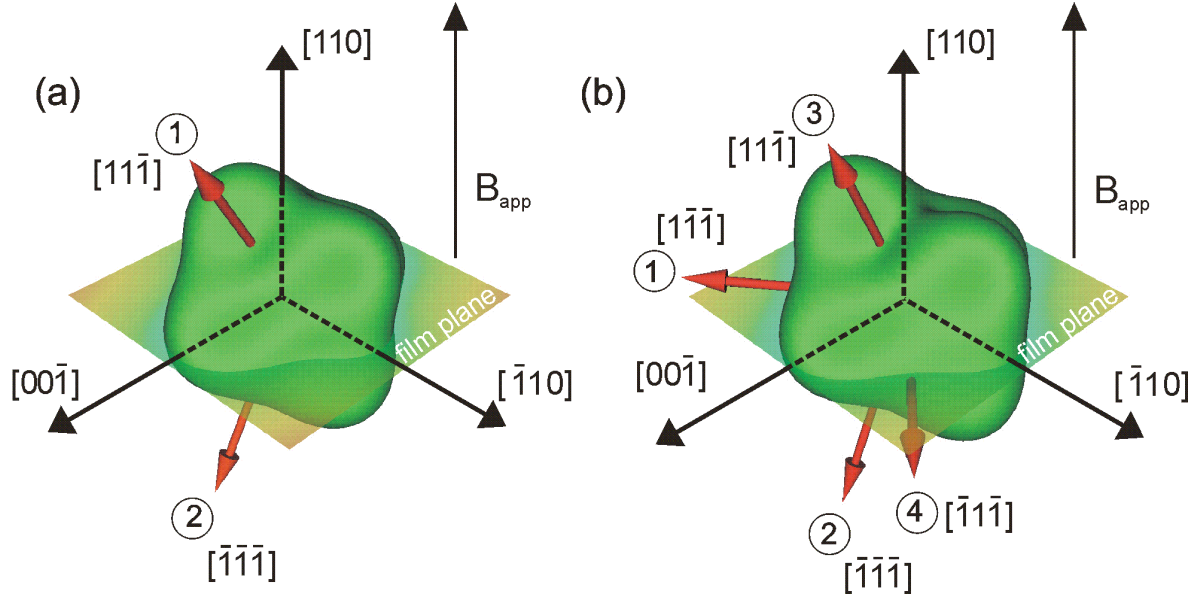


**Fig. 2.** Calculated anisotropy energy surfaces for the  $\text{ErFe}_2$  layers at (a) 100 K and (b) 200 K. The arrows indicate the average direction of the  $\text{ErFe}_2$  moment as the applied field is swept from a high positive to negative value. At 100 K arrow 1 (2) corresponds to an applied field of +15 T (-15 T). At 200 K arrow 1 (4) corresponds to an applied field of +7.52 T (-7.52 T) and arrow 2 (3) corresponds to an applied field of +3.04 T (-3.04 T).

We interpret the experimental and micro-magnetic data as follows. Below  $T_{\text{CO}}$  there are only two directions in which the  $\text{ErFe}_2$  magnetisation can point. In a high magnetic field they point out of plane, somewhere between the  $[11\bar{1}]$ -axis and the applied field along the  $[110]$ -axis. But as  $B_{\text{app}}$  is decreased, the Er moments move closer to the  $[11\bar{1}]$  axis, under the action of the strong Er magneto-crystalline anisotropy. Finally, in a sufficiently high negative field, the Er moments switch to align along an ‘inverse’ out of plane, say the  $[\bar{1}\bar{1}\bar{1}]$ -axis. In summary, the Er and Fe spins are confined to the  $[11\bar{1}]-[110]$  plane by the strong Er magneto-crystalline energy and there is just one switching event.

Above  $T_{\text{CO}}$  there are four directions in which the average  $\text{ErFe}_2$  moment can point. In a high magnetic field, OOMMF calculations reveal that the average  $\text{ErFe}_2$  magnetisation lies almost perpendicular to the applied field, close to one of the in-plane  $\langle 111 \rangle$ -axes e.g. the  $[\bar{1}\bar{1}\bar{1}]$ -axis. We call this an exchange spring driven spin-flop transition. Here the Er moments take advantage of one of the four in-plane magneto-crystalline local minima. Note that all the moments are confined, primarily, to the  $[\bar{1}\bar{1}\bar{1}]-[110]$  plane (c.f. the  $[11\bar{1}]-[110]$  plane at low temperatures). However, as the field is decreased the average the  $\text{ErFe}_2$  magnetisation rotates both *downwards and sideways* to the  $[\bar{1}\bar{1}\bar{1}]-[\bar{1}\bar{1}0]$  plane, roughly opposite to the applied field. This rotation is driven by (i) the dominant  $\text{YFe}_2$  magnetisation, (ii) the weakening of the Er anisotropy energy, and (iii) the overall out-of-plane minimum in the Er anisotropy. This rotation signals the first step in the hysteresis loop. On reducing the field to a relatively modest negative value, the  $\text{ErFe}_2$  layers switch again to point out of plane

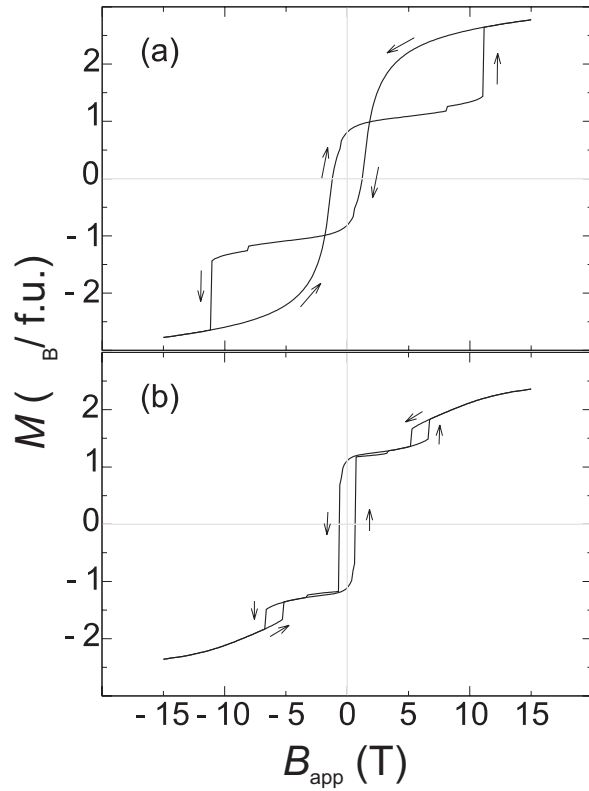


**Fig. 3.** Hysteresis curves for  $[\text{ErFe}_2(50 \text{ \AA})/\text{YFe}_2(150 \text{ \AA})] \times 20$  at (a) 100 K and (b) 200 K, obtained using OOMMF.  $B_{app}$  is parallel to the  $[110]$  growth axis.

nearly opposite the applied field direction, but still in the  $[\bar{1}\bar{1}0]-[\bar{1}\bar{1}\bar{1}]$  plane. This constitutes the second irreversible step, which can be viewed as simple switching of the soft  $\text{YFe}_2$  magnetisation. Finally, in a high negative field the third and final irreversible step occurs as the  $\text{ErFe}_2$  magnetisation rotates to take up the exchange spring driven spin-flop state, but this time with the  $\text{YFe}_2$  moments in the opposite direction.

## References

- <sup>1</sup> E. E. Fullerton, J. S. Jiang, M. Grimsditch, C. H. Sowers and S. D. Bader, *Phys. Rev. B* **58**, 12193 (1998).
- <sup>2</sup> E. E. Fullerton, J. S. Jiang and S. D. Bader, *J. Magn. Magn. Mater.* **200**, 392 (1999).
- <sup>3</sup> R. Skomski and J. M. D. Coey, *IEEE Trans. Magn.* **29**, 2860 (1993).
- <sup>4</sup> R. Skomski and J. M. D. Coey, *Phys. Rev. B* **48**, 15812 (1993).
- <sup>5</sup> D. Suess, T. Schrefl, R. Dittrich, M. Kirschner, F. Dorfbauer, G. Hrkac and J. Fidler, *J. Magn. Magn. Mater.* **290**, 551 (2005).
- <sup>6</sup> R. H. Victora and X. Shen, *IEEE Trans. Magn.* **41**, 537 (2005).
- <sup>7</sup> D. Suess, T. Schrefl, S. Fahler, M. Kirschner, G. Hrkac, F. Dorfbauer and J. Fidler, *Appl. Phys. Lett.* **87**, 12504 (2005).
- <sup>8</sup> K. Dumesnil, M. Dutheil, C. Dufour and Ph. Mangin, *Phys. Rev. B* **62**, 1136 (2000).
- <sup>9</sup> S.N. Gordeev, J-M. L. Beaujour, G. J. Bowden, B. D. Rainford, P. A. J. de Groot, R. C. C. Ward, M. R. Wells and A. G. M. Jansen, *Phys. Rev. Lett.* **87**, 186808 (2001).
- <sup>10</sup> K. Dumesnil, C. Dufour, Ph. Mangin, F. Wilhelm and A. Rogalev, *J. Appl. Phys.* **95**, 6843 (2004).
- <sup>11</sup> Z. Tun, W. J. L. Buyers, I. P. Swainson, M. Sutton and R. W. Cochrane, *J. Appl. Phys.* **76**, 7075 (1994).
- <sup>12</sup> V. Oderno, C. Dufour, K. Dumesnil, Ph. Mangin and G. Marchal, *J. Cryst. Growth* **165**, 175 (1996).
- <sup>13</sup> M. Sawicki, G. J. Bowden, P. A. J. de Groot, B. D. Rainford, R. C. C. Ward and M. R. Wells, *J. Appl. Phys.* **87**, 6839-41, (2000).
- <sup>14</sup> M. J. Donahue and D. G. Porter, *OOMMF Users Guide* (National Institute of Standards and Technology, Gaithersburg, MD, 1999), interagency report NISTIR 6376.
- <sup>15</sup> J-M. L. Beaujour, S. N. Gordeev, G. J. Bowden, P. A. J. de Groot, B. D. Rainford, R. C. C. Ward and M. R. Wells, *Appl. Phys. Lett.* **78**, 964 (2001).
- <sup>16</sup> M. Sawicki, G. J. Bowden, P. A. J. de Groot, B. D. Rainford, J-M. L. Beaujour, R. C. C. Ward and M. R. Wells, *Phys. Rev. B* **62**, 5817 (2000).
- <sup>17</sup> U. Atzmony and M. P. Dariel, *Phys. Rev. B* **13**, 4006 (1976).
- <sup>18</sup> A. Mougin, C. Dufour, K. Dumesnil, N. Maloufi, Ph. Mangin and G. Patrat, *Phys. Rev. B* **59**, 5950 (1999).
- <sup>19</sup> A. Mougin, C. Dufour, K. Dumesnil and Ph. Mangin, *Phys. Rev. B* **62**, 9517 (2000).
- <sup>20</sup> W. F. Brown Jr., *Micromagnetics* (Interscience, New York (1963)
- <sup>21</sup> B. D. Cullity *Introduction to Magnetic Materials, Addison-Wesley Pub. Comp* (1972) p402.